

Original article

**Measurement and modelling
of the photosynthetically active radiation
transmitted in a canopy of maritime pine**

P Hassika*, P Berbigier, JM Bonnefond

*Laboratoire de bioclimatologie Inra, domaine de la Grande-Ferrade, BP 81,
33883 Villenave-d'Ornon cedex, France*

(Received 20 May 1996; accepted 20 May 1997)

Summary – Modelling the photosynthesis of a forest requires the evaluation of the quantity of photosynthetically active radiation (PAR) absorbed by the crowns and the understorey. In this article a semi-empirical model, based on Beer's law is used to study PAR absorption and its seasonal variation. Our purpose was to confirm that the PAR and the solar radiation follow the same interception laws for both the direct and diffuse part, using correct values of needle transmission and reflection coefficients. The model developed took into account the direct and the diffuse radiation. The radiation rescattered by the crowns was neglected following an estimation using the Kubelka–Munk equations, which indicated that the term was small. The model was calibrated and tested from the measurements taken in a maritime pine forest during the summer and autumn of 1995. The comparison between the results of the model and the measurements was satisfactory for the direct radiation as well as for the diffuse radiation. In conclusion, although the measurement wavebands are different, the penetration of the PAR can be estimated using the same simple semi-empirical model already established for solar radiation.

model / solar radiation / photosynthetically active radiation / penetration / maritime pine

Résumé — **Mesure et modélisation du rayonnement utile à la photosynthèse transmis dans un couvert de pin maritime.** Pour la modélisation de la photosynthèse d'un couvert végétal, il est important de connaître la quantité de rayonnement utile à la photosynthèse (PAR) absorbé par les couronnes et le sous-bois. Dans cet article, un modèle semi-empirique, exploitant la loi de Beer, ainsi que les variations saisonnières du PAR sont présentés. L'objectif de l'étude est de confirmer que le rayonnement utile à la photosynthèse et le rayonnement solaire suivent les mêmes lois d'interception pour le direct et pour le diffus en intégrant les valeurs mesurées de réflectance et de transmittance. Le modèle établi prend en compte le rayonnement direct et le rayonnement diffus. Le rayonnement

* Correspondence and reprints
Tel: (33) 05 56 84 31 87; fax: (33) 05 56 84 31 35; e-mail: hassika@bordeaux.inra.fr

rediffusé par le houppier est estimé à partir des équations de Kubelka-Munk. Lorsque ce terme est négligé, on montre que l'erreur induite sur le bilan radiatif est faible. Les entrées du modèle sont déduites des mesures effectuées sur une forêt de pin maritime durant l'été et l'automne 1995. La comparaison entre les résultats du modèle et les mesures est satisfaisante aussi bien pour le rayonnement direct que pour le rayonnement diffus. En conclusion, bien que les ordres de grandeurs et les domaines spectraux des mesures soient différents, la pénétration du rayonnement utile à la photosynthèse peut être estimée par un simple modèle semi-empirique déjà établi pour le rayonnement solaire.

modèle / rayonnement solaire / rayonnement utile à la photosynthèse / pénétration / pin maritime

INTRODUCTION

Studying the evapotranspiration and the photosynthesis of plants is useful in many fields, such as plant physiology, biomass production on a large scale and interaction with the overall climate of the earth. When extrapolating from a foliage element to the whole plant, the interception profile of radiation has the largest vertical gradient, and is thus essential for scaling-up. In forest canopies, in contrast, vertical gradients of temperature, concentration of water vapour and CO_2 are very low. The photosynthetic activity depends first of all on the photosynthetically active radiation (PAR) intercepted and the combined effects of water vapour concentration and air temperature. Internal CO_2 concentrations in the intercellular spaces of the leaves and the water stress of the canopy also play a role (Jones, 1992).

The numerous interception models of radiation by plants vary from simple modelling based on Beer's law (Bonhomme and Varlet-Grancher, 1977) to more complex models characterized by a discretization of the canopy into elementary volumes or cells. These cells have a known geometrical shape and a known location in space. In general, these models do not take the multiple scattering between these different cells into account. These cells can be ellipsoids (Norman and Welles, 1983), cones (Wang and Jarvis, 1990), rows of cylinders and cones (Jackson and Palmer, 1972), ellipsoids (Charles-Edwards and Thorpe, 1976), or

parallelepipeds (Sinoquet, 1993). A Monte-Carlo simulation can be used to calculate the direct solar radiation at different points in a canopy (Oker-Blom, 1984).

However, very few studies have focused on the photosynthetically active radiation (PAR) of the solar spectrum (Sinclair and Lemon, 1974; Sinclair and Knoerr, 1982; Pukkala et al, 1991). Other teams (Alados et al, 1995; Papaioannou et al, 1996) have studied the relationship between the PAR and the solar radiation. These studies tend to show that the ratio between the PAR and the solar radiation depends on solar elevation, sky conditions and dewpoint temperature. Spitters et al (1986) also established an empirical relationship between global and diffuse PAR.

In this paper we applied the model developed by Berbigier and Bonnefond (1995) for solar radiation on a forest canopy (Les Landes, France) to the PAR. The objective of this model is to predict the proportion of direct and diffuse PAR reaching the understorey using measurements of incident global and diffuse PAR above the canopy. This very simple semi-empirical model represents the canopy as a horizontally homogeneous diffusing layer. The direct and diffuse radiation penetrates according to Beer's law. The scattered radiation is estimated from the Kubelka-Munk (1931) equations, which have also been used by Bonhomme and Varlet-Grancher (1977). This model is semi-empirical since the extinction coefficient is adjusted from measurements.

The outputs of the model were validated using data collected during a series of measurements in summer and autumn 1995.

In this paper we divide the global PAR or incident PAR into a direct part (direct PAR) and a diffuse part (diffuse PAR). The reflected to incident PAR ratio will be called PAR reflectance.

MATERIAL AND METHODS

Experimental data were collected during summer 1995 in a maritime pine forest planted in 1969. The plantation is located 20 km south-west of Bordeaux (latitude 44° 42' N, longitude 0° 46' W).

On a 1-ha stand, the trees were planted in parallel rows. The mean height of the trees was approximately 16 m. The maximum height was 18 m and the mean height of the bases of the crowns was 9 m. Tree density was 660 trees per hectare. The soil was completely covered with clumps of grass approximately 0.7 m high, which were completely green at the time of measurements. In a first approximation this forest can be described by two distinct plant layers, ie, the crowns of the pines and the gramineae of the understorey. The trees were planted along an axis NE–SW. The leaf area index (LAI) varied between 3.4 and 3 during the measurement season (July–October). This LAI was measured using a Démon system (Lang, 1987), according to the method proposed by Lang et al (1991) where the total surface area index was estimated from gap frequencies. These frequencies were deduced from the penetration of direct sunbeams. This method is based on Cauchy's theorems (Lang, 1991).

Measurements of the photosynthetically active radiation

The tools generally used for measuring PAR are cells containing crystalline silicon, such as those manufactured by Licor (LI 190S), which respond almost instantaneously to small or sudden variations in light intensity.

For this experiment, 25 cells were prepared in the laboratory using the method developed by Chartier et al (1993). These sensors delivered a

voltage proportional to the incident radiation. To measure this potential difference we used a resistance of 18 ohms. To reduce the specular reflection, a tarnished filter, which only allowed the spectrum between 400 and 700 nm to pass, was stuck above each cell.

A number of sensors were mounted above the canopy on a 25-m-high scaffolding. At this level at the end of a 2-m-long rod, two cells, one facing upward and the other downward, measured the global PAR and the reflected PAR.

On the same site, at 2 m above the ground and at the top of the scaffolding, two cells locally measured the diffuse PAR below and above the canopy, respectively. The diffuse PAR was obtained by using a shadow band, which stopped the direct PAR. The error induced on the measurement was small: to account for the effect of the part of the sky vault hidden by the shadow band, a multiplier of 1.084 given by the manufacturer was applied.

At 1 m above the ground, a trolley rolling at a speed of 2 m/min on a 22-m railway parallel to the row carried five two-sided (one facing upward and one facing downward) sensors located on a transversal rod whose length was equal to the width of the inter-row (4 m). Every 15 min this experimental device calculated the mean of the values measured every 10 s (Bonfond, 1993). This system allowed us to perform a space–time average of the measurements and to smooth the effect of the rows.

Cells were calibrated against a CM11, Kipp and Zonen thermopile during very clear weather and at maximum solar elevation. Under these conditions it is possible to calibrate quantum sensors against solar energy sensors because the spectrum distribution of the solar energy remains constant (Varlet-Grancher et al, 1981). In international units (SI) the density of the solar energy flow is measured in watts per square meter ($\text{W}\cdot\text{m}^{-2}$). The flux density of the PAR (photosynthetic photon flux density (PPFD): 400–700 nm) is usually defined in moles of photons per surface unit and per unit of time ($\text{photon}\cdot\text{m}^{-2}\cdot\text{s}^{-1}$). We found that, in the case of clear days, $2.02 \mu\text{mol m}^{-2} \text{s}^{-1}$ of PAR were equal to $1 \text{ W}\cdot\text{m}^{-2}$ of global radiation.

All sensors had similar calibration coefficients. In order to avoid any measurement error due to sensor failure (ageing, loss of sensitivity, contact defect) a new calibration was made under similar conditions at the end of the season. Results appeared to be identical.

In parallel with PAR measurements, the net and global radiation above the forest as well as its PAR reflectance were measured for the whole solar spectrum (table I).

Data were recorded on a data acquisition system of the Campbell 21X type (Campbell Scientific, Logan, UT). As for the mobile measurements, the recorded values were the 15-min average of measurements taken every 10 s.

For this study we had a complete set of measurements (direct and diffuse PAR at the lower and higher levels) for clear days 189 and 193. For days 275, 279, 280 and 281 (clear sky) the measurement of the lower diffuse radiation was missing.

We also had a complete set of measurements for two days with a partially or totally overcast sky (190 and 192).

Lastly, for days 247, 249, 250, 265–273, 276–278 and 282 (totally or partially overcast days) the measurement of the lower diffuse PAR was missing, whereas for days 187, 188, 191 and 194–198 the measurement of the lower global PAR was missing.

The direct PAR above the canopy $R_b(0)$ was obtained by the difference between the measurements of the diffuse and global PAR above the canopy: $R_b(0) = R_g(0) - R_d(0)$.

THEORY

The forest of Les Landes is modelled as two well-separated plant layers, ie, the understorey and the crowns. We focused on the amount of PAR transmitted through the crown layer.

This theory has already been developed for solar radiation, by Berbigier and Bonnefond (1995). The aim of the model is to calculate the PAR transmitted and absorbed from measurements of the incident direct and diffuse PAR.

Non-intercepted direct PAR

The non-intercepted direct PAR is simply modelled by Beer–Bouguer's law, which can be written as:

$$R_b(\lambda) = R_b(0) \exp(-K\lambda / \sin\beta) \quad [1]$$

where $R_b(\lambda)$ ($\mu\text{mol m}^{-2} \text{s}^{-1}$) is the direct PAR at a given level within the crown, $R_b(0)$ is the direct PAR above the canopy, λ is the LAI integrated from the top of the canopy to the point where $R_b(\lambda)$ is defined, β is the solar elevation angle and K a non-dimensional extinction coefficient. When the whole crown is considered, $\lambda = L$ is the LAI of the canopy. Thus, when using Beer's law, the only parameter required is the extinction coefficient (K) of the canopy.

Non-intercepted diffuse PAR

Distribution laws of luminance corresponding to clear or overcast lighting conditions are very different. For the sake of simplicity we used the standard overcast

Table I. Radiation sensors used during the experiment. For this paper we only use the photosynthetic measurements.

<i>Radiation measurement</i>	<i>Instrument</i>	<i>Waveband (μm)</i>	<i>Manufacturer and model</i>
Short-wave incoming	Pyranometer	0.285–2.8	Kipp and Zonen Model CM5
Allwave net	Net radiometer	0.3–60	Inra
Photosynthetic incoming	Silicon cells	0.4–0.7	Solems
Photosynthetic outgoing	Inverted silicon cells	0.4–0.7	Solems
Photosynthetic diffuse	Silicon cells with shadowband	0.4–0.7	Solems

sky (SOC) law proposed by Steven and Unsworth (1980). For clear weather, strictly speaking this law is not correct because there is a strong circumsolar diffuse PAR. However, since the diffuse PAR represents only approximately 15% of the global PAR, this error is acceptable as a first approximation.

The expression of this law proposed by Steven and Unsworth (1980) is:

$$N(\beta, \phi) = \{N(\pi/2) / 2.23\} \{1 + 1.23 \sin\beta\} \quad [2]$$

where $N(\beta, \phi)$ is the luminance value, $N(\pi/2, 0)$ the luminance value at zenith and the angular source azimuth. $R_d(0)$ is the measured value of the incident diffuse PAR. As a consequence of equation [2], the density of the diffuse PAR above the canopy is written:

$$R_d(\lambda) = \frac{R_d(0)}{0.91} \int_0^1 \exp(-K\lambda/u) (1 + 1.23u) u du \quad [3]$$

where $u = \sin\beta$.

This integral has no analytical solution. However, its numerical value can be closely adjusted to a function $Y = \exp(-K'\lambda)$ using the least-squares method (Berbigier and Bonnefond, 1995). We obtained $K' = 0.467$.

Scattered PAR

Measurements showed that the diffuse PAR reaching the understorey is spatially homogeneous even in a discontinuous canopy. As with the non-intercepted PAR, the rescattered radiation can be treated a fortiori with the hypothesis that the canopy is continuous.

The method consists in writing the radiation balance of an elementary horizontal layer with a thickness $d\lambda$. The rescattered radiation depends on the reflectance and the transmittance of the foliage elements (ρ and τ) as well as on the PAR reflectance of the understorey. Reflectance (ρ) and transmittance (τ) in the PAR waveband on needles of

maritime pines have already been measured by Berbigier and Bonnefond (1995)

$$\rho = 0.090 \quad \tau = 0.014 \quad [4]$$

The scattered radiation was deduced for each elementary layer, when the radiation balance is integrated from $\lambda = 0$ to $\lambda = L$. These values made it possible to obtain the total diffuse PAR of the crown (Bonhomme and Varlet-Grancher, 1977; Sinoquet et al, 1993).

The analytical solution of these equations was given by Bonhomme and Varlet-Grancher (1977) for a canopy of maize when $\rho = \tau$ and by Berbigier and Bonnefond (1995) for a canopy of maritime pines when $\rho \neq \tau$. We used the solution established by the last authors.

RESULTS AND DISCUSSION

Experimental measurements

Figure 1 shows the different terms of the radiation balance in the PAR above and below the canopy for clear weather (day 193) as a function of the hour of the day. The transmission of the incident PAR varies with the solar elevation and is much lower for low incident angle incidences. Apart from a cloudy period at approximately 1400 hours UT, which explains the fall in the global PAR and the increase in the incident diffuse PAR, the curves show the expected shape. The incident global PAR reached a maximum of approximately 1900 $\mu\text{mol}\cdot\text{m}^{-2}\cdot\text{s}^{-1}$ in the middle of the day. The global PAR below the crowns reached a peak at approximately 700 $\mu\text{mol}\cdot\text{m}^{-2}\cdot\text{s}^{-1}$ around 1300 hours (denoted '1' in fig 1), which corresponds to the presence of the sun between the rows. The effects of the two adjacent rows of crowns can also be seen on the measurements (denoted '2' in fig 1).

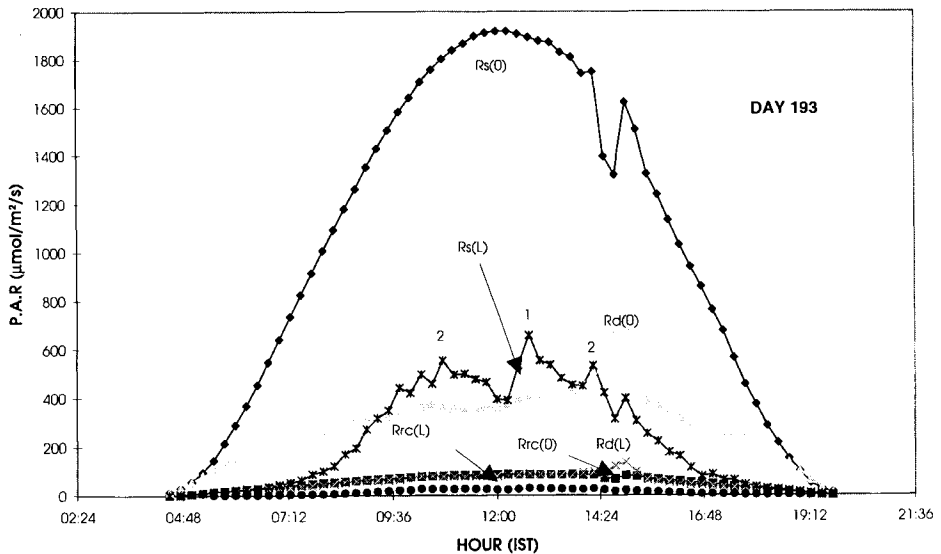


Fig 1. An example of PAR measurement on a sunny day, above and under the canopy. *Above the canopy:* PAR (global): $R_s(0)$; sky diffuse PAR: $R_d(0)$; PAR reflected: $R_{rc}(0)$. *Under the canopy:* PAR (global): $R_s(L)$; understory diffuse PAR: $R_d(L)$; PAR reflected by grass: $R_{rc}(L)$.

To estimate the scattered PAR it is necessary to know the PAR reflectance of the understory. This PAR reflectance is defined as the ratio between incident PAR and reflected PAR. An example of variations with time for a day of measurements of the PAR reflectance of the canopy and the understory is presented in figure 2.

The increase in the canopy PAR reflectance at the beginning and at the end of the day is due to the interception of the top of the plant canopy. For this day the average PAR reflectance above this forest reached approximately 0.06. This value represents less than half of the PAR reflectance of the solar radiation when the whole spectrum is taken into account (fig 2). Although this value seems low, this result is coherent with another study (Gash et al, 1989).

For the understory PAR reflectance the values at the beginning and the end of the day are not representative because the values

of the reflected PAR are extremely low (less than $3 \mu\text{mol m}^{-2} \text{s}^{-1}$). When the understory average PAR reflectance could be measured, it reached approximately 0.05.

The daily value of the canopy PAR reflectance is defined as the ratio between the sum of daily incident PAR and the sum of daily reflected PAR above the canopy. We deduce PAR reflectance and the ratio of incident diffuse PAR on incident global PAR by using the daily sums, since the direct PAR depends more closely on the solar elevation angle.

In figure 3a a regular increase in the canopy PAR reflectance was observed on the forest, during the seasonal measurement. The forest PAR reflectance reached approximately 0.05 at the beginning of July and 0.07 at the beginning of October. This increase could be due to the increased stand reflectivity at low incidences, which has

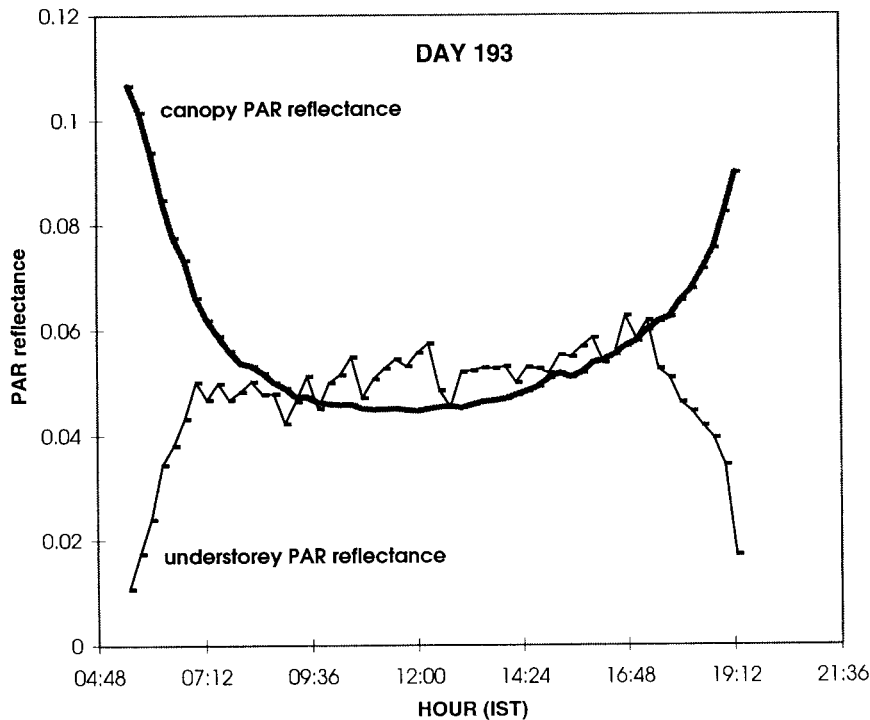


Fig 2. An example of daily variation of the forest PAR reflectance and the understorey PAR reflectance for a clear day (day 193).

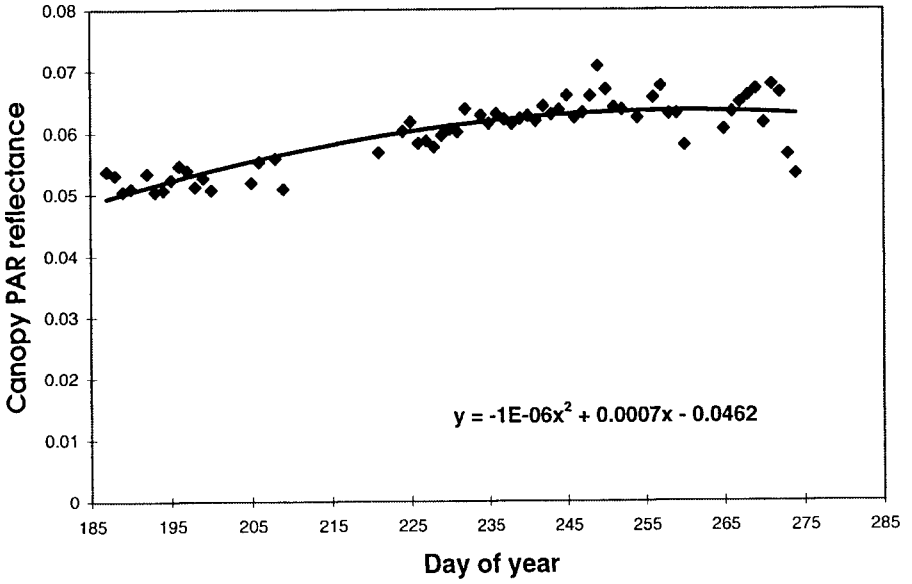
already been mentioned, and perhaps to the death of 3-year old needles.

Figure 3b shows the variation curve of the understorey PAR reflectance. A maximum can be observed in the mean value between days 235 and 255. This increase was possibly due to a short period of water deficiency in the summer of 1995: the gramineae were dry and had lost their green colour unlike the needles which remained green. After rainfall, a decrease was observed. The mean forest and understorey PAR reflectance was 0.06 and 0.05, respectively, over this period. These two values of the PAR reflectance are not additive because the reflected PAR above the canopy is not the sum of the PAR reflected by the understorey and crowns.

Variations in diffuse PAR and global PAR daily means are presented in figure 4 for the period from 5 July to 9 October 1995 (days 186–282). It shows a divergence between the trends of the global and the diffuse PAR, probably due to the mean decrease in solar elevation. Since the ratio between the diffuse and global PAR presents more intra-day variations, we do not show a curve of the 15-min ratios, which were much more variable.

Table II shows the values of the proportions between the diffuse PAR and the global PAR, which were measured for clear and variable weather throughout the season. For clear days the density of the diffuse PAR represented approximately 15% of the global PAR. This ratio was 40% for the variable

a)



b)

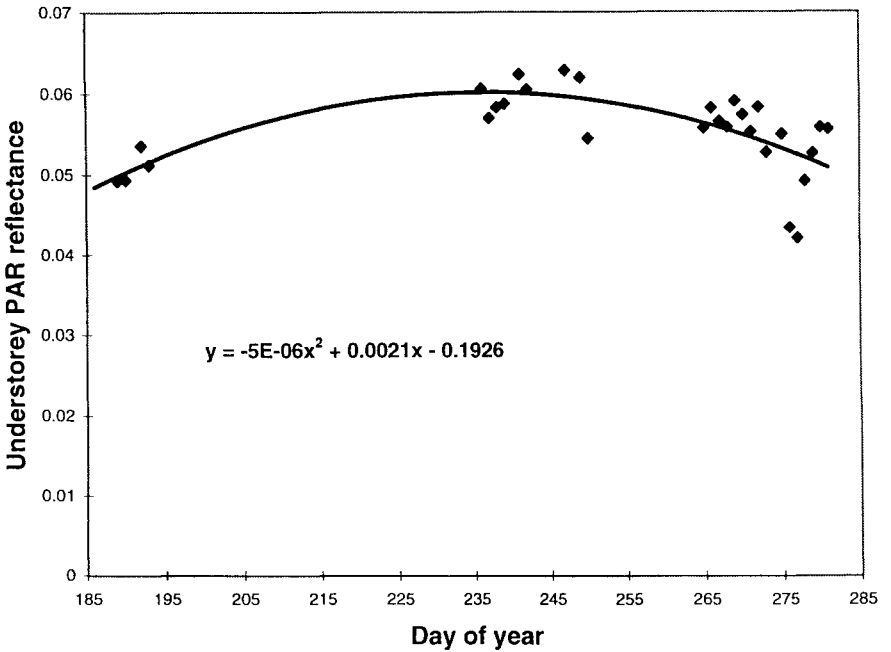


Fig 3. Seasonal variation of the PAR reflectance of the forest (a) and the understorey (b).

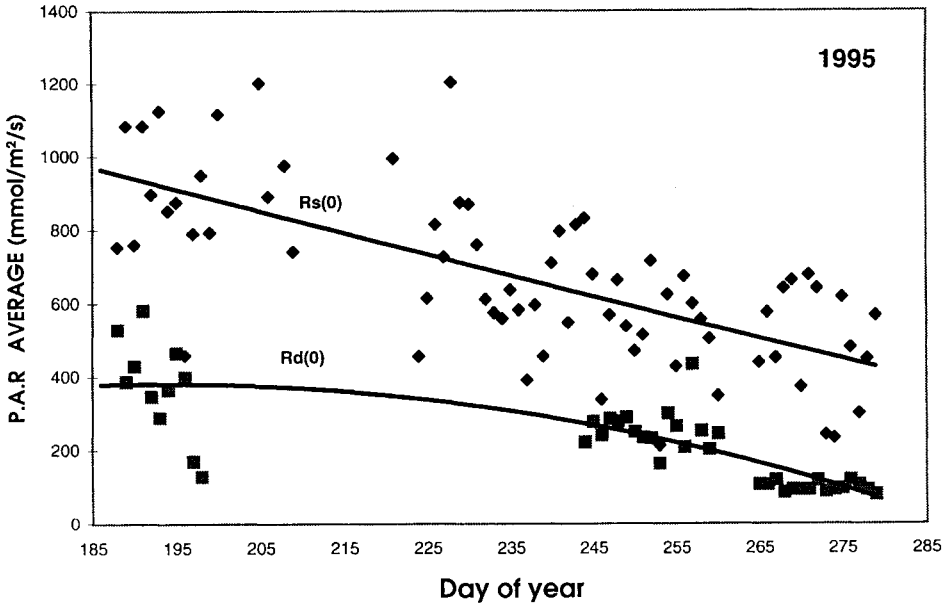


Fig 4. Seasonal variations of the average global $R_s(0)$ and the diffuse $R_d(0)$ PAR.

Table II. Ratio of diffuse to global PAR for solar elevation angles greater than 30°. The mean values of these ratios are deduced by using the sum of daily measurements.

	<i>Total diffuse radiation/total global radiation above the canopy</i>		<i>Number of observations</i>
	<i>Mean values</i>	<i>Standard deviations</i>	
Days of clear sky (189, 193, 243, 244, 275, 279, 280, 281)	0.1542	0.0879	372
Days of variable sky (192, 194–199, 245–260, 265–278 and 282)	0.4033	0.0523	502
All the days between 189 and 282	0.3011	0.0236	1407

days and 30% for all the days. These values imply that the proportion of diffuse PAR in the global PAR was almost equivalent to the proportion of diffuse radiation in the global solar radiation.

This result has to be compared to other studies (Efimova, 1967) which suggest that

the PAR can be estimated from measurements of radiation with short wavelengths using the following relation:

$$\text{global PAR} = 0.43 (\text{direct PAR}) + 0.57 (\text{diffuse PAR})$$

The difference observed in our study (30% versus 57% in the former) can be explained by the fact that our study was performed during a rather sunny part of the year. A more precise estimation of these values is currently being studied.

However, since measuring the diffuse PAR routinely is relatively complicated, it is also of interest to search for a semi-empirical relation between the diffuse PAR and the global PAR, which could avoid measuring the diffuse PAR. Spitters et al (1986) also established an empirical relationship between global and diffuse PAR, taking into account sunshine duration. Unlike the solar radiation this type of relation has never been established for PAR in our region. This relationship is currently being studied in our laboratory.

Modelling

The model was adjusted on three days with clear and overcast sky (days 189, 190, 192)

for which all the data were available. These days were chosen close to the summer solstice in order to have a maximum variation in the solar height. The different parts of the model were then validated with the corresponding measurements of the other days between days 188 and 282.

Direct radiation

The extinction coefficient K of the foliage elements can be deduced from Beer's law and written as:

$$K = \frac{\sin(\beta)}{\text{LAI}} \ln \left(\frac{R_b(\lambda)}{R_b(0)} \right) \quad [5]$$

where $R_b(0)$ and $R_b(\lambda)$ represent the direct PAR below and above the crowns, respectively. In figure 5 a relationship between K and the angles of solar elevation is observed. Strictly speaking, K cannot be assumed constant since it varies with sun angular elevation (de Wit, 1965).

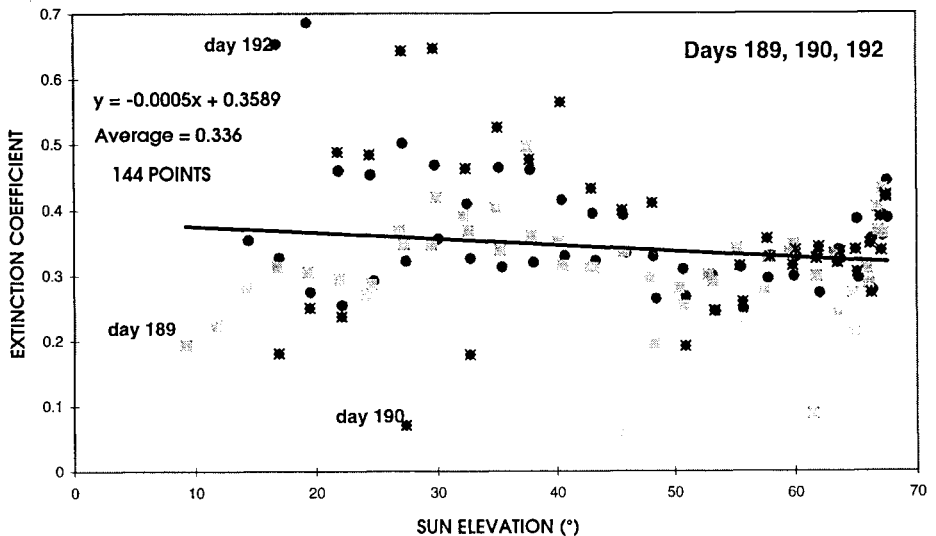


Fig 5. Variation of the extinction coefficient K as a function of the sun elevation angle for days 189, 191 and 192.

On days 189, 190 and 192 K was calculated for solar elevation angles greater than 30° . The mean values are given in table III. The overall average is:

$$K = 0.33 \pm 0.103 \quad [6]$$

On the same experimental site Berbigier and Bonnefond (1995) have found the same value in a study of solar radiation. Consequently, with the same hypotheses, Beer's law in this forest has a unique extinction coefficient for the PAR as well as the solar radiation.

However, without assuming that the foliage index is horizontally homogeneous, the effect of the angular distribution of the needle must be included. Nevertheless we checked this using the ellipsoidal distribution of the needle orientations suggested by Campbell (1986). This did not give better results, which justifies the use of a constant K .

Figure 6a shows a comparison between the measurements of the direct PAR and the modelled direct PAR using equation [6] on day 193. Variations in the direct PAR in the understorey resulting from the presence of rows cannot be seen from the results of the model, which is based on the assumption of a continuous horizontal canopy.

Figure 6b gives an example of the outputs of the model to direct PAR measurements on day 189. It compares the mea-

surements and the outputs of the model for one of the days used to adjust equation [1]. The deviations to the model are represented with a linear regression forced to the origin. The slope of this line is 0.95 for $R^2 = 0.9$. An increasing dispersion is observed for the high values, which is due to rows.

However, figure 7 shows that the comparison between all the measurements of all the days not used to adjust the model and the outputs of the model may be represented with a linear regression forced to the origin. It can be noted that the model slightly overestimates the measurements since the slope of this line is 0.96 for $R^2 = 0.91$. This bias may result from the hypothesis of a constant K , which does not exactly represent the reality.

Diffuse PAR

The diffuse PAR measured below the canopy is the sum of the sky diffuse PAR having crossed the canopy without being intercepted and the PAR scattered by the elements of the crown. We first studied the scattered part of the PAR.

The model is applied for evaluating the scattered PAR to all the days. The values obtained are lower than $5 \pm 0.025 \mu\text{mol}\cdot\text{m}^{-2}\cdot\text{s}^{-1}$ on average, ie, less than 4% of the lower diffuse radiation.

These values are within the range of absolute error of our sensors. Consequently,

Table III. Extinction coefficient deduced by inverting Beer's law (days 189, 190 and 192). These values are deduced by using all measurements.

Days	Extinction coefficient K		Number of observations
	Daily values	Standard deviations	
189	0.358	0.091	47
190	0.349	0.139	45
192	0.307	0.078	47
mean	0.33	0.103	139

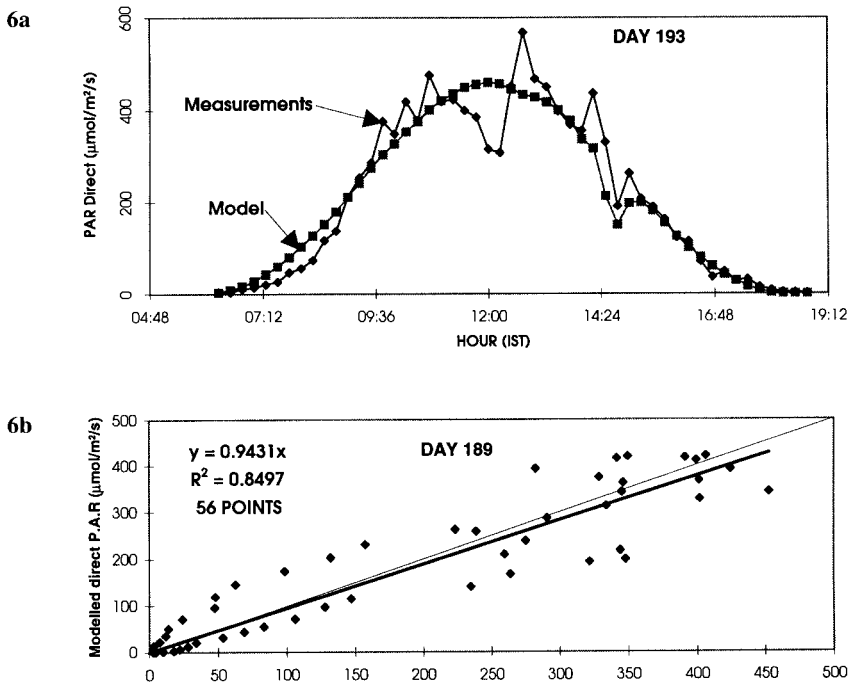


Fig 6. Comparison between the outputs of the model with measurements of the direct PAR on two days close to the solstice (days 193 and 189): (a) daily variation of non-intercepted direct PAR; (b) regression line of day 189.

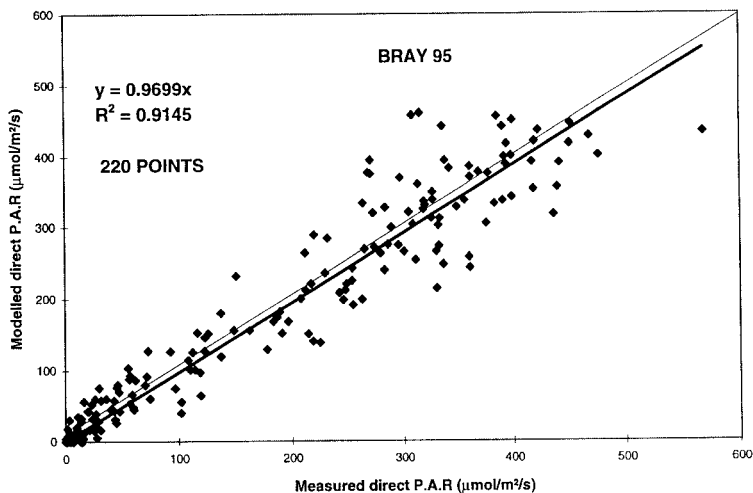


Fig 7. Comparison between modelled direct PAR and measured direct PAR for all measurement days.

this part can be neglected when modelling the radiation transmitted because the error induced is lower than 1% on the estimation of the global radiation in the understory. The rescattered radiation is not accounted for in the model.

It was shown above (equation [3]) that the non-intercepted diffuse PAR $R_d(\lambda)$ at depth λ can be written as:

$$R_d(\lambda) = R_d(0) \exp(-0.467\lambda) \quad [7]$$

Regarding measurements and the simulation of day 193 (fig 8a), the orientation of the rows does not seem to affect the proportion of diffuse PAR transmitted to the understory. The simulation example shown in fig 8a was made on a clear day (except from 1400 to 1500 IST) in order to suppress the disruptive effects of the clouds.

Figure 8b shows that the diffuse PAR is homogeneous. Thus, the diffuse radiation smooths the effect of the rows. A linearity defect between the measurements and the model can be seen. This bias may result from the hypothesis of a constant K , which would affect K' . However, this angle was observed on clear days, where the diffuse PAR was very small ($150 \mu\text{mol}\cdot\text{m}^{-2}\cdot\text{s}^{-1}$ at maximum).

The model was validated on all the days not used to adjust the K coefficient and for which the lower diffuse PAR was measured. Predictions were in agreement with the measurements and the maximum difference with the line 1:1 was approximately $26 \mu\text{mol}\cdot\text{m}^{-2}\cdot\text{s}^{-1}$ (fig 9).

Global PAR

The outputs of the complete model can now be compared to the measurements of the global PAR (fig 10) for all the experimental days where this measurement is available (1 350 points). A good agreement is observed ($R^2 = 0.94$) in spite of a slight

underestimation (slope 0.9), which may be due to geometrical effects of the crowns (rows, holes, preferential orientations of the foliage elements).

CONCLUSION

Since the penetration of the PAR into plant canopies is poorly documented, we tried, in this paper, to apply a semi-empirical model to the PAR. This model was previously established for the solar radiation in a forest of maritime pines. The daily variations of the incident and transmitted PAR were presented.

A regular increase in the canopy PAR reflectance was observed, during the measurement season. This value, approximately 0.05 at the beginning of July, reached 0.065 in October. During the same time, for understory PAR reflectance an increase in the mean value between days 235 and 255 could be observed. This increase was due to a short period of water deficiency. Later we showed that the reflectivity of the canopy was much lower in the PAR than for the whole solar waveband.

The proportions between the diffuse PAR and the global PAR, which were measured by clear and variable weather throughout the season, were compared. The diffuse PAR represented approximately 30% of the global PAR.

The outputs of the model of the direct PAR and the diffuse PAR transmitted to the soil showed a good correlation with the seasonal measurements. This result enables us to state that this model is a good tool for predicting the interception of the PAR in the forest, ie, the partition of PAR between crowns and understory.

In a first approximation, the extinction coefficient K is constant. The daily outputs of the model of the direct PAR and the diffuse PAR transmitted to the soil were not in agreement with measurements, but more

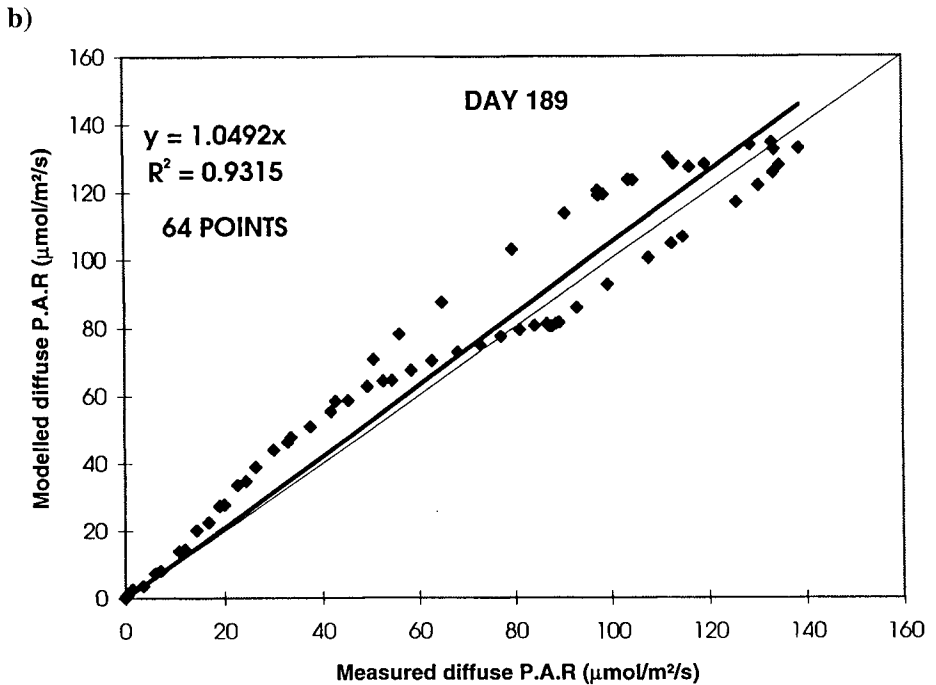
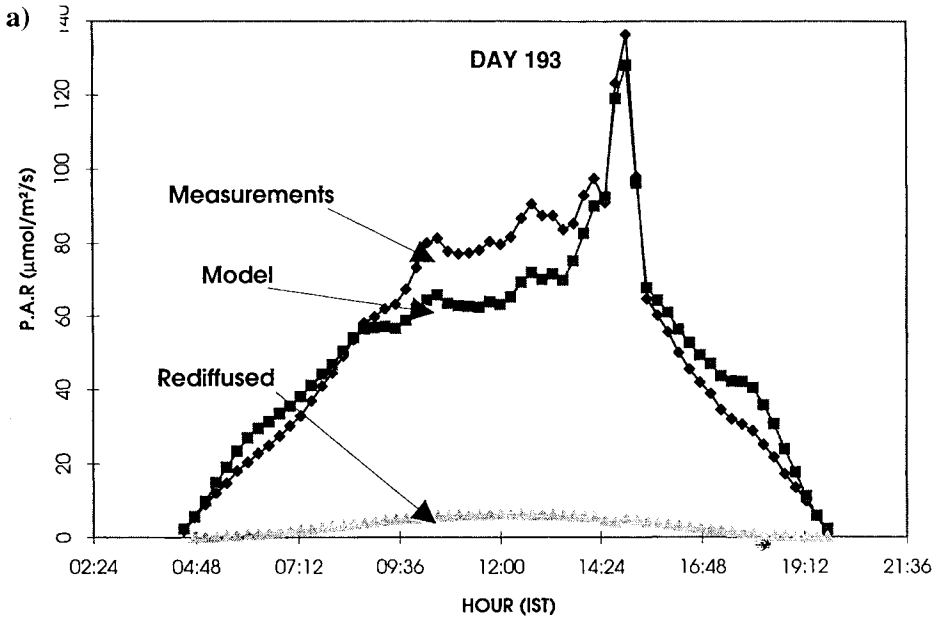


Fig 8. Comparison between the outputs of the model with measurements of the understorey diffuse PAR on a day at the beginning of the season close to the solstice (days 193 and 189): (a) daily variation of non-intercepted diffuse PAR; (b) regression line of day 189.

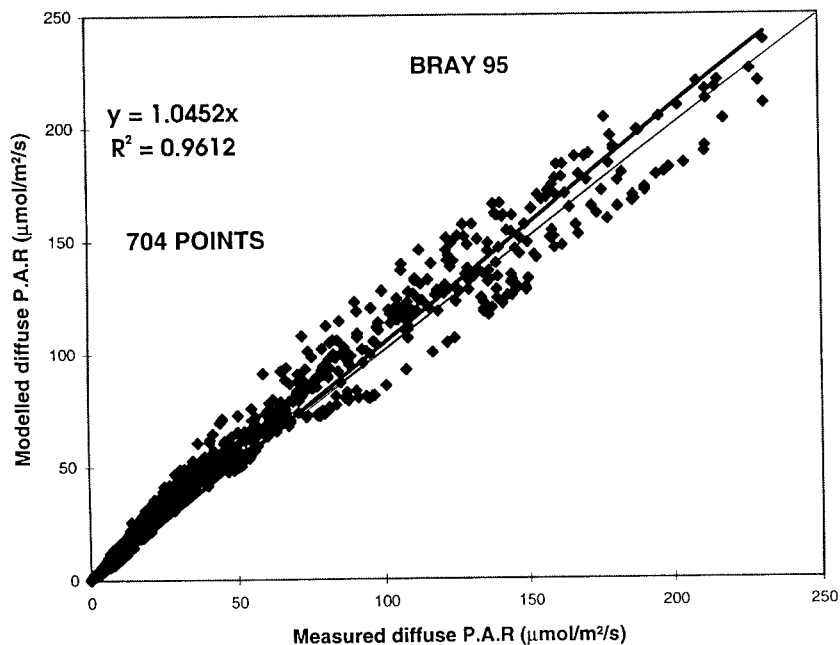


Fig 9. Comparison between modelled diffuse PAR and measured diffuse PAR for all measurement days.

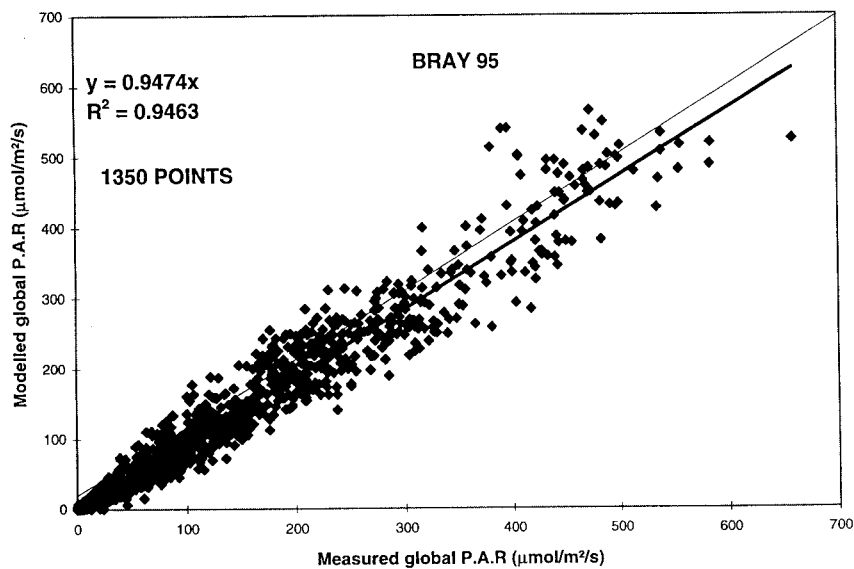


Fig 10. Comparison between modelled global PAR and measured global PAR by using all the data available between days 189 and 282. The values of the model are the sums of the estimated direct PAR and the estimated diffuse PAR.

realistic models of K will be tested afterwards.

Nevertheless, this model may be useful for ecophysiological studies.

Acknowledgements: The authors thank Y Brunet, I Champion and M Irvine for proof-reading this article as well as A Kruszewski for constructing and installing sensors on the experimental site. This work was partially supported by the Conseil regional of Aquitaine.

REFERENCES

- Alados I, Foyo-Moreno I, Alados-Arboledas L (1995) Photosynthetically active radiation: measurements and modelling. *Agric For Meteorol* 78, 121-131
- Berbigier P, Bonnefond JM (1995) Measurement and modelling of radiation transmission within a stand of maritime pine (*Pinus pinaster* Ait). *Ann Sci For* 52, 23-42
- Bonhomme R, Varlet-Grancher C (1977) Application aux couverts végétaux des lois de rayonnement en milieu diffusant. I. Établissement des lois et vérifications. *Ann Agro* 28, 567-582
- Bonnefond JM (1993) Études d'un système mobile destiné à la mesure du rayonnement. Application à la mesure du rayonnement global et du rayonnement net sous un couvert de pins maritimes. *Cah Tech Inra* 30, 13-32
- Campbell GS (1986) Extinction coefficients for radiation in plant canopies calculated using an ellipsoidal inclination angle distribution. *Agric For Meteorol* 36, 317-321
- Charles-Edwards DA, Thorpe MR (1976) Interception of diffuse and direct-beam radiation by a hedgerow apple orchard. *Ann Bot* 44, 603-613
- Chartier M, Allirand JM, Varlet-Grancher C (1993) Canopy radiation balance: its components and their measurement. In: *Crop Structure and Light Microclimate* (C Varlet-Grancher, R Bonhomme, H Sinoquet, eds), Inra Versailles, France, 29-43
- Efimova N (1967) Photosynthetically active radiation over the USSR. In: *Plant Photosynthetic Production Manual of Methods* (Z. Sestak, J Catsky, PG Jarvis, eds), Dr W. Junk NV, 412-466
- Gash JHC, Shuttleworth WJ, Lloyd CR, André JC, Goutorbe J-P, Gelpe J (1989) Micrometeorological measurements in les Landes forest during Hapex-Mobilhy. *Agric For Meteorol* 46, 131-147
- Jackson JE, Palmer JW (1972) Interception of light by model hedgerow orchards in relation to latitude, time of year and hedgerow configuration and orientation. *Appl Ecol* 9, 341-357
- Jones HG (1992) Photosynthesis and respiration. In: *Plants and Microclimate. A Quantitative Approach to Environmental Plant Physiology*, 2 ed. Cambridge Univ Press, Cambridge
- Kubelka P, Munk F (1931) Ein Beitrag zur Optik der Farbanstriche. *Zeits Furtechn Physik* 12, 593
- Lang ARG (1987) Simplified estimate of leaf area index from transmittance of the sun's beam. *Agric For Meteorol* 41, 179-186
- Lang ARG, McMurtie RE, Benson ML (1991) Validity of surface area indices of *Pinus radiata* estimated from transmittance of the sun's beam. *Agric For Meteorol* 55
- Lang ARG (1991) Application of some of Cauchy's theorems to estimation of surface areas of leaves, needles and branches of plants, and light transmittance. *Agric For Meteorol* 55, 191-212
- Norman JM, Welles JM (1983) Radiative transfer in an array of canopies. *Agron J* 75, 481-488
- Oker-Blom P (1984) Penumbral effects of within-plant and between-plant shading on radiation distribution and leaf photosynthesis: a Monte-Carlo simulation. *Photosynthetica* 18, 522-528
- Papaioannou G, Nikolidakis G, Asimakopoulos D, Retalis D (1996). Photosynthetically active radiation in Athens. *Agric For Meteorol*, 81, 287-298
- Pukkala T, Becker P, Kuuluvainen T, Oker-Blom P (1991) Predicting spatial distribution of direct radiation below forest canopies. *Agric For Meteorol* 55, 295-307
- Sinclair TR, Lemon ER (1974) Penetration of photosynthetically active radiation in corn canopies. *Agron J* 66, 201-205
- Sinclair TR, Knoerr KR (1982) Distribution of photosynthetically active radiation in the canopy of a loblolly pine plantation. *J Appl Ecol* 19, 183-191
- Sinoquet H (1993) Modelling radiative transfer in heterogeneous canopies and intercropping systems. In: *Crop Structure and Light Microclimate* (R Bonhomme, C Varlet-Grancher, H Sinoquet, eds), Inra, Versailles, France, 229-252
- Spitters CJT, Tousaint HAJM, Goudriaan J (1986). Separating the diffuse and direct component of global radiation and its implications for modelling canopy photosynthesis. Part I. Components of incoming radiation. *Agric For Meteorol* 38, 217-229
- Steven MD, Unsworth MH (1980) The diffuse irradiance of slopes under cloudless skies. *QJR Meteorol Soc* 105, 593-602
- Varlet-Grancher C, Chartier M, Gosse G, Bonhomme R (1981) Rayonnement utile pour la photosynthèse des végétaux en conditions naturelles : caractérisation et variations. *Acta Oecol Plant* 16, 189-202
- Wang YP and Jarvis PG (1990) Description and validation of an array model MAESTRO. *Agric For Meteorol* 51, 257-280
- de Wit CT (1965) Photosynthesis of leaf canopies. Agricultural Research Report No 663, Center for Agricultural publication and documentation, Wageningen, the Netherlands